INDIAN JOURNAL OF SCIENCE AND TECHNOLOGY

RESEARCH ARTICLE

# Evaluation of Antioxidant and Antibacterial Property of Microwave Assisted Green Synthesis of $Fe_3O_4$ -MgO Nanocomposites

**Lakkappa B Anigol[1], Vinodkumar P Sajjan[1], Prabhuodeyara M Gurubasavaraj[1]***

**1** Department of Chemistry, Rani Channamma University, Vidyasangama, PBNH-04, Belagavi, 591156, Karnataka, India

OPEN ACCESS

**Received:** 18-03-2023

**Accepted:** 01-06-2023

**Published:** 19-06-2023

**Citation:** Anigol LB, Sajjan VP, Gurubasavaraj PM (2023) Evaluation of Antioxidant and Antibacterial Property of Microwave Assisted Green Synthesis of $Fe_3O_4$ -MgO Nanocomposites. Indian Journal of Science and Technology 16(24): 1777-1786. https://doi.org/10.17485/IJST/v16i24.629

* **Corresponding author**.

pmg@rcub.ac.in

**Funding:** The work was financially supported by Karnataka DST-Ph.D. fellowship of Department of Science and Technology (DST), Govt. of Karnataka. (No: DST/KSTePS/Ph.D fellowship/CHE-05:2020-21) KSTePS, DST, Government of Karnataka, Bangalore to the first author. PMG thanks to VGST (GRD 503 & 952) and Rani Channamma University for Minor research project 2020 & 2021

**Competing Interests:** None



Published By Indian Society for Education and Environment (iSee)

**ISSN**
Print: 0974-6846
Electronic: 0974-5645

## Abstract

**Objectives:** To synthesize Magnesium oxide, iron oxide nanoparticles and $Fe_3O_4$-MgO nanocomposite using agro waste of lemon peel extract (LPE) and to examine their antioxidant and antibacterial activity. **Methods:** MgO, $Fe_3O_4$ NPs and $Fe_3O_4$–MgO nanocomposite by microwave-assisted technique using LPE. Feature techniques such as UV-Visible spectroscopy, X-ray diffraction (XRD), Thermo gravimetric analysis (TGA) and Scanning electron microscope (SEM) were performed to characterize the prepared material in terms of morphology and structure. Furthermore, Fourier transform infrared (FTIR) spectroscopy analysis was used to identify the possible functional groups present in the synthesis of MgO, $Fe_3O_4$NPs and $Fe_3O_4$-MgO nanocomposite. **Finding:** Powder XRD confirmed the formation of MgO, $Fe_3O_4$ NPs and $Fe_3O_4$-MgO nanocomposite, SEM analysis confirmed that Iron oxide and Magnesium oxide nanoparticles and $Fe_3O_4$-MgO nanocomposite are mostly in spherical shape, while TG analysis indicated the greater thermal stability of nanoparticles as well as nanocomposite. All Synthesized nanoparticles and nanocomposite showed good antibacterial activity against gram positive and gram-negative bacterial strains ($IC_{50}$ value are 8.32, 8.15 & 8.13 and 7.23, 7.57 & 7.47 $\mu$g/mL respectively). These metal oxide NPs showed antioxidant activities against DPPH (less than 85%) but enhancing activity was found for $Fe_3O_4$-MgO nanocomposite (89.95%). **Novelty:** These results suggested that LPE derived $Fe_3O_4$-MgO nanocomposites can be used as an effective antioxidant and antibacterial agent in biomedical applications.

**Keywords:** Lemon Peels Extract; Green Synthesis; Nanocomposites; Antioxidant Activity; Hemolytic Assay; Antibacterial Activity

## 1 Introduction

Metal oxide nanoparticles have been synthesized by green synthesis in previous works with different plant extracts, mainly by *Citrus reticulata* (orange) bark extract,

*Murraya koenigii* (Curry leaves), hydrated extract of *Curcuma longa* (turmeric) *Jatropha curcus L.* leaf extract and *Azadirachta indica* (Neem) leaf juice extract[1]. Lemons are recommended to speculate on distinct biological activities, including antioxidant, antiallergic soothing, anti-proliferative, anti-mutagenic and anticancer activity[2]. This leads to search for a new class of nanoparticles which are non-toxic and able to utilize in biological activities. To the best of our knowledge, reports on main group and transition metal nanocomposites using LPE agro waste are elusive.

The evaluation of the antioxidant and antibacterial activity of nanomaterials has become one of the important fundamental studies in pharmaceutical science as well as nanoscience and technology. In the functioning of all biological systems, antioxidant and antibacterial properties play an important role. In biological systems, free radicals are generated by the interaction of biomolecules with molecular oxygen. These free radicals are responsible for the degradation of biomolecules. Oxidation is also the cause of loss of nutritional quality and food discoloration[3]. The consumption of oxidized foods produces lipid peroxides and low molecular weight compounds that cause serious diseases such as hepatomegaly or necrosis of epithelial tissues. In biological systems, antioxidants play an important role in scavenging these toxic free radicals.

To date, a variety of natural and synthetic antioxidants have been studied to inhibit these oxidative reactions. Saikia et al.[4] reported that $Fe_3O_4$ and NiO nanoparticles had good antioxidant activity. Banerjee et al.[5] reported that nanostructured materials are expected to act as better free radical scavengers than their bulk materials, wherever there is material interaction. This property is due to the high surface/volume ratio of the nanostructures. In the mammalian system, hemolysis is an observable event of destruction of red blood cells (RBCs) resulting in the release of hemoglobin into the surrounding fluid. This hemoglobin release can be distinguished by spectroscopic analysis. Severe hemolysis can lead to dangerous medical conditions. Therefore, all biomedical products intended for intravenous administration should be evaluated for their hemolytic properties[6]. So, in this article we report the synthesis of $Fe_3O_4$-MgO nanocomposites using agricultural waste and its application in biological activity.

### 1.1 Research Gap

Nanomaterials are ideal candidates for biomedical and environmental treatment applications that gained too many attentions due to their high sorption capacity and facile access in the separation stages and recovery. Researchers from all over the world have worked hard to design and produce green synthesized nanoparticles. According to Prasad et al.[7], in order to remove an organic dye from aqueous media, they created super magnetic Ni-$Fe_3O_4$nanocomposites using the extract from *Moringa oleifera* leaves, where the extract served as a reducing and capping agent. In order to reduce nitroarenes Sajadi et al.[8] created Cu/$Fe_3O_4$nanocomposites using *Silybum marianum* L. extract. According to their observation, the plants C=O and C-O functional groups were crucial in capping the nanoparticles that were created. In a different study by Prasad et al. created a green and cost-effective method for producing reduced graphene oxide (rGO) combined with magnetite nanoparticles (rGO-$Fe_3O_4$) in order to remove lead oxide (Pb (II)) from aqueous medium utilizing *Murraya koenigii* leaves extract. Along with the research on composite nanoparticles mentioned above, these useful nanoparticles can also be used as catalysts for organic transformation in liquid medium, the complete recovery of pollutants from waste waters[9] and hydrogenation catalysis[10]. These applications highlight the significance of these nanomaterials and the need for their development using environmentally friendly methods. Here, we report the evaluation of antibacterial and anti-oxidant properties of $Fe_3O_4$-MgO nanocomposite using a simple, inexpensive, eco-friendly, and green process employing agricultural waste lemon peel extract. Lemon peel extract demonstrated wonderful potential to enhance antibacterial and antioxidant performance despite the majority of green techniques.

In this paper, an attempt was made to synthesize of MgO, $Fe_3O_4$ NPs and $Fe_3O_4$–MgO nanocomposites by microwave-assisted technique and examine its antioxidant and antibacterial activity. The antioxidant activity of the synthesized MgO, $Fe_3O_4$NPs and $Fe_3O_4$–MgO nanomaterial was evaluated by a free radical scavenging assay with individually variable nanoparticle concentrations and time intervals. An *in vitro* hemolysis test was also performed to evaluate the biocompatibility of these nanoparticles and nanocomposites to ensure their potential application in biomedicine.

## 2 Methodology

### 2.1 Materials

All chemicals are reagent grade and used without further purification $FeSO_4.7H_2O$ and Mg $(NO_3)_2.6H_2O$ were purchased from Aldrich, India. Distilled water was used in all experiments. All glass wares was washed with an acid/base solution, followed by distilled water and finally dried in a hot air oven.

## 2.2 Preparation of lemon peel extract

Lemon peels were collected from the Belagavi market and washed several times with running water and then with double distilled water to remove dust particles. About 50 grams of dry lemon peel was cut into small pieces and placed in a 500 ml conical flask containing 200 ml of distilled water and heated at 75-80°C for 4 hours. The obtained pale yellow filtrate was separated from the particulate matter by filtration with whatman No. 1 and lemon peel extract (LPE) were stored at 4°C for further testing.

## 2.3 Green synthesis of MgO NPs

To synthesize green MgO NPs, 4 mM of Mg $(NO_3)_2.6H_20$ was added to 50 ml of distilled water and 50 ml of prepared lemon peel extract was added to the reaction mixture and maintained with vigorous magnetic stirring for 5 hours. The visual color change from a yellowish to white precipitate indicates that MgO NPs have formed [11]. The obtained MgO NPs were centrifuged at 12,000 rpm for 2×20 min and washed several times with 1:1 mixture of distilled water and absolute ethanol. Finally, the purified MgO NPs powder was dried at 90°C for 10 hours and calcinated at 500°C for 5 hours and stored in an airtight bottle for further characterization.

## 2.4 Green synthesis of $Fe_3O_4$ NPs

For the green synthetic $Fe_3O_4$NPs, 4 mM of $FeSO_4.7H_20$ was added to 50 ml of distilled water. 50 ml of the prepared lemon peel extract was added to the reaction mixture and vigorously stirred for 5 hours. The visual color change of the precipitate from yellow to brown indicates that formation of $Fe_3O_4$NPs [12]. The obtained iron oxide NPs was centrifuged at 12,000 rpm for 2×20 min and washed several times with 1:1 mixture of distilled water and absolute ethanol. Finally, the purified $Fe_3O_4$NPs powder was dried at 90°C for 10 hours and calcinated at 500°C for 5 hours and stored in an air tight bottle for further characterization.

## 2.5 Preparation of $Fe_3O_4$–MgO nanocomposites

The binary composite of iron and magnesium oxide was synthesized by microwave method using MgO NPs and $Fe_3O_4$ NPS with 1:1 ethanol and water. This was put in a microwave oven and exposed to microwave radiation for 10 minutes at strength of 800 W and a frequency of 2450 MHz. The resulting mixture was centrifuged at 12,000 rpm for 2×20 min and washed with 1:1 mixture of distilled water and absolute ethanol. Finally, dry it in a hot air oven for 12 hours at 95°C and calcinated at 550°C for 6 hours to obtain the $Fe_3O_4$–MgO nanocomposite and stored in an airtight bottle for further characterization using FTIR, XRD and TGA.

## 2.6 Analytical characterization of nanomaterials

Optical properties of samples containing lemon peel extract of MgO, $Fe_3O_4$NPs and $Fe_3O_4$-MgO nanocomposites were confirmed by single-beam UV-visible spectrophotometer (Shimadzu, UV-1800). The crystal phase of the prepared samples was determined using X-ray diffraction (XRD) (Rigaku Minifex, Difractometer). Reflective mode with Cu K$\alpha$ radiation at 30 kV and a scan rate of 2% min and a scan range of 10° to 80° ($2\theta$) is used. The FT-IR spectra of the prepared nanoparticles were analyzed in the 4000-400 $cm^{-1}$range using a Fourier transform infrared (FT-IR) (Thermo Scientifc, Nicolet iZ10). The detection of functional groups helps to analyze the structural changes occurring in the nanocomposites. The thermal stability and decomposition temperature of the nanoparticles and nanocomposites samples were evaluated by thermo gravimetric analysis (TGA) (TA-SDT650, USA). The sample (4.5-5 mg) was heated over a temperature range of 25-500°C at an increment of 10°C/min in a nitrogen atmosphere. SEM images of the nanoparticles were taken with a JEOL – JSM – 6390LV scanning electron microscope.

## 2.7 Cytotoxicity measurement by hemolytic assay

Hemolysis essentially involves the release of hemoglobin in plasma due to damage to the erythrocyte membrane. Here, the hemolytic activity assay was performed for MgO NPs, $Fe_3O_4$ NPs and $Fe_3O_4$–MgO nonmaterial according to the procedure of Neun et al. [13] with light change. An 8-mL sample of human blood from a volunteer following consent was collected in $K_3$EDTA tube and then 8-mL of blood sample and 1 mL of 3.8% sodium citrate is added to inhibit coagulation. Then the sample is centrifuge in a centrifuge tube at 3000 rpm for 5 min. The supernatant containing platelet-poor plasma is removed and tablets containing red blood cells re-suspended in 10 ml of phosphate buffered saline (PBS) with pH 7.4. This process is repeated two to three times to completely remove the buffer from the red blood cells. Finally, the cells were suspended in PBS

to get a uniform suspension of cells. MgO NPs, $Fe_3O_4$ and $Fe_3O_4$–MgO nonmaterial were placed in different test tubes. Then 2-ml erythrocyte suspensions were added to each test tube. The tubes are then rotated slightly to maintain contact blood with nanoparticles and incubated at 37 °C for 90 min. Positive and negative controls were prepared by adding the same amount of red blood cell suspension in Triton X–100 and PBS (pH-7.4), respectively. After incubation, the samples were centrifuged at 3000 rpm for 5 min to form pelleted red blood cells. Upper part then carefully separated and used for absorption studies at 540 nm using a UV-vis spectrophotometer against a PBS blank solution. Percentage of hemolysis is expressed using the following formula.

$$\text{Hemolysis}\ (\%) = \frac{(\text{OD test samples - OD negative control})}{(\text{OD positive control- OD negative control})} \times 100$$

Where OD is the optical density

### 2.8 Antioxidant activity (AOA)

The antioxidant activities of MgO NPs, $Fe_3O_4$ NPs and $Fe_3O_4$–MgO nanomaterials were assessed based on free radical scavenging activity by DPPH method. DPPH stock solution was prepared by dissolving 3.9432 mg of DPPH in 100 ml of methanol and stored at 4°C until use. 2 ml of DPPH solution was mixed with 1 ml of five different concentrations (20, 40, 60, 80 and 100 $\mu g\ mL^{-1}$) of the nanomaterial and standard, respectively. A mixture of 1 ml of distilled water and 2 ml of DPPH solution was used as a control. The reaction mixture was well mixed and kept in the dark for 30 min and incubated at room temperature. Absorbance was recorded photometrically at 517 nm. The antioxidant activity was estimated based on the percentage of DPPH radicals retained according to the following equation.

$$\text{Scavenging effect}\ \% = \frac{\text{Control absorbance} - \text{Sample absorbance} \times 100}{\text{Control absorbance}}$$

### 2.9 Antibacterial activity (Nutrient agar media)

The well agar diffusion method was used to assess the antibacterial activity of MgO, $Fe_3O_4$ NPs, and $Fe_3O_4$-MgO nanocomposites against gram-positive (*Staphylococcus aureus and S. mutans*) and gram-negative (*Escherichia coli and Klebsiella pneumonia*) bacteria. Peptone (20 g), beef extract (5.0 g), sodium chloride (5 g), and agar (20 g) were combined with 1 L of distilled water to create the nutrient agar medium. The pH was adjusted to 7.2 to 7.4 before sterilization in an autoclave at 120°C for 20 minutes at 15 lbs of pressure. After being placed to the Muller Hinton agar plate, the agar nutrient medium was used to culture a bacterial lawn. The nanocomposites at a concentration of 50 g/ml were added to this and incubated at 37 °C for 24 h. Furthermore, the possible results were analyzed on the basis of zone of inhibition in millimeter using vernier calliper. In the current investigation, Ciprofloxacin was also employed as a standard.

## 3 Results and Discussion

### 3.1 UV–Vis spectroscopy

The formation and stability of metal nanoparticles are demonstrated by UV-vis spectroscopy because the solution containing the nanoparticles exhibit an absorption band in the UV-vis region as a result of the surface plasmon oscillation of the metal electrons. This absorption band also offers information on the size and shape of the metal nanoparticles[14]. In this study, the visual transition of color change indicates the formation of MgO NPs and $Fe_3O_4$NPs mediated by lemon peel and $Fe_3O_4$-MgO nanocomposites. The biosynthesized metal oxide NPs illustrated absorbance peaks in the range of 200–300 nm. The appearance of surface plasmon resonance (SPR) band at shorter wavelengths below 300 nm specifies the existence of small sized particles[15]. The SPR peak obtained at 280, 278 and 276 nm were in the range of 270 and 280 nm confirmed the formation of phytosynthesized nanoparticles of MgO NPs and $Fe_3O_4$NPs mediated by lemon peel and $Fe_3O_4$-MgO nanocomposite respectively (Figure 1). The obtained SPR peak confirmed the phytoreduction of Mg $(NO_3)_2$ to MgO NPs and $FeSO_4.7H_2O$ to $Fe_3O_4$NPs[16]. It was clear that the phytochemicals are present in the lemon peel may function as a reducing, capping and stabilizing agent towards the phytosynthesis of metal oxide nanoparticles.

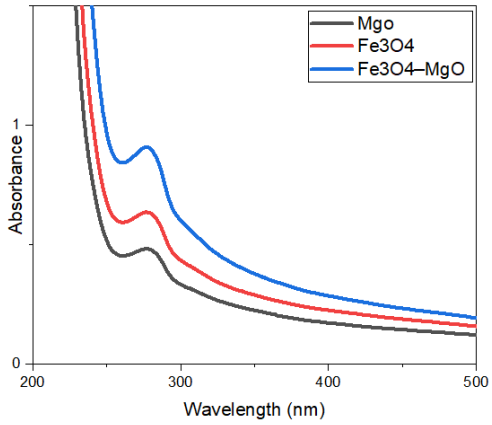


**Fig 1.** UV-Vis spectra of MgO, $Fe_3O_4$ NPs and $Fe_3O_4$-MgO nanocomposite

## 3.2 Fourier Transform Infrared (FT-IR ) Spectroscopy

FTIR spectroscopy was used to identify the respective chemical groups and it can explain the existences of surface functional groups in metal interactions present in the synthesized metal oxide nanoparticles of lemon feel extract. The band at 3449 $cm^{-1}$ was assigned to O–H group which may belong to water or plant phenolic compounds. The occurrence of peak at 2929 and 2920 $cm^{-1}$ confirmed C–H group in MgO NPs and $Fe_3O_4$NPs respectively. The bands at 1628, 1638 $cm^{-1}$ and 1228 $cm^{-1}$ attributed to C=O and C–H group respectively. The IR peak at 504 $cm^{-1}$ corresponds to Mg–O stretching frequency of MgO and the peak at 620 $cm^{-1}$ ascribed to Fe–O stretching vibrations of $Fe_3O_4$. Furthermore, the FTIR spectra of $Fe_3O_4$-MgO nanocomposite exhibit the presence of both Mg–O and Fe–O vibration peaks in the range of 724-562 $cm^{-1}$ it confirms the formation of nanocomposite (Figure 2).

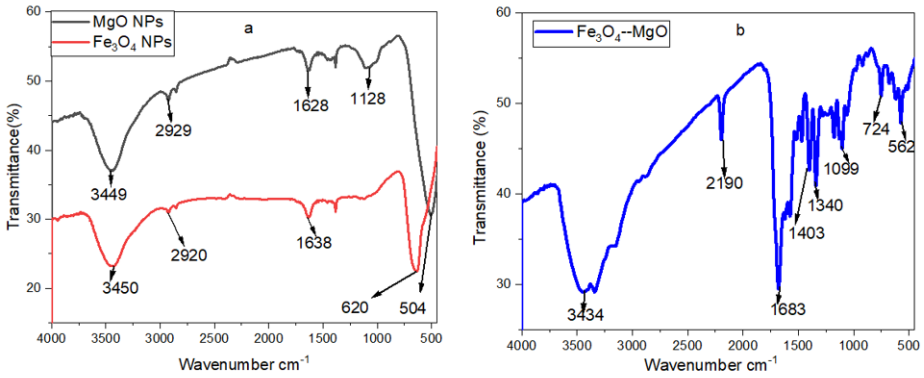


**Fig 2.** FT-IR spectra of a) MgO, $Fe_3O_4$NPs and b) $Fe_3O_4$-MgO nanocomposite

## 3.3 X-ray Diffraction (XRD Analysis

The crystallinity, structure and phase of the synthesized nanomaterials were analyzed using XRD. Figure 3 shows the XRD patterns of the prepared MgO, $Fe_3O_4$ nanoparticles and $Fe_3O_4$-MgO nanocomposites. From the XRD, formation of face centered cubic phase MgO crystal was confirmed by (JCPDS card No: 01-1235)[17]. The $2\theta$ values of MgO at 32, 42, 62, 75 and 78 corresponds to (111), (200), (220), (311) and (222) were referring to cubic crystal structure. Further $Fe_3O_4$ apparent peaks were observed at 29, 36, 39, 43, 57 and 64 degrees which corresponds to (2 2 0), (3 1 1), (2 2 2), (4 0 0), (5 1 1) and (4 4 0) face centered cubic crystal orientation, respectively[18]. Sharp peaks were observed XRD patterns of $Fe_3O_4$ which indicate that pure $Fe_3O_4$ NPs. The XRD pattern of $Fe_3O_4$-MgO composite shows the characteristic peaks of both MgO and $Fe_3O_4$. The X-ray diffractogram reveals the well crystalline nature of the nanocomposites.

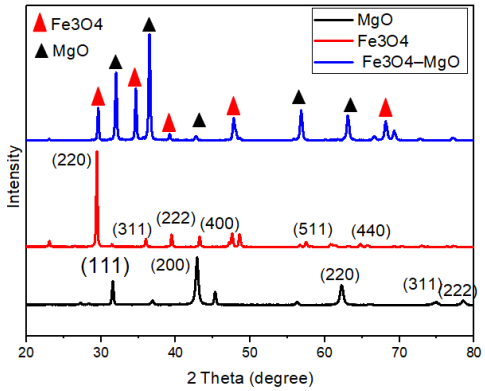


**Fig 3.** XRD spectra of MgO, $Fe_3O_4$NPs and $Fe_3O_4$-MgO nanocomposite

## 3.4 Scanning Electron Microscopy (SEM)

In order to understand the morphologies of MgO, $Fe_3O_4$ NPs and $Fe_3O_4$-MgO nanocomposites were performed using scanning electron microscopy. Figure 4 illustrates the MgO, $Fe_3O_4$ NPs and $Fe_3O_4$-MgO nanocomposites. SEM images revealed that the synthesized MgO NPs were agglomerated and formed small cubic structured nanoparticles. Such morphology may be attributed to the fact that, the free ions ($NO^{3-}$, $OH^{-}$) might have adsorbed on the crystallographic plane of the solid sample surface through weak coordination with $Mg^{+2}$ ion or through hydrogen bonding, during the synthesis of the nanomaterials [19]. SEM images of $Fe_3O_4$ NPs were formed in cubic structures. It was also seen in the SEM images that $Fe_3O_4$ nanoparticles agglomerated due to their magnetic properties. SEM images of $Fe_3O_4$-MgO nanocomposites are also presented in Figure 4. Visual inspections revealed that the combination of MgO NPs and $Fe_3O_4$NPs in the microwave irradiation makes the shape of $Fe_3O_4$-MgO composite material spherical in nature.

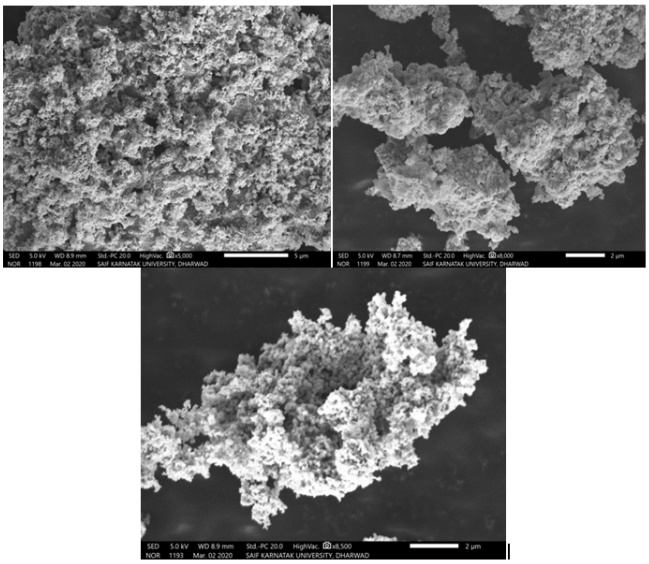

**Fig 4.** SEM images of MgO, $Fe_3O_4$ NPs and $Fe_3O_4$-MgO nanocomposite

## 3.5 Thermo gravimetric Analysis (TGA)

The thermal behaviors of MgO, $Fe_3O_4$ and $Fe_3O_4$-MgO nanocomposite were characterized by thermo gravimetric analysis (TGA) and the results are shown in Figure 5. The TGA of MgO was obtained in normal atmospheric conditions, with heating rate of 10 °C /min. The analysis indicated the loss of mass occurred in two steps; the first step is from 25°C to 260°C, which may

due to the liberation of water molecules adsorbed on the surface. The second step occurs in the range of 260°C to 450°C, which may be dehydroxylation of Mg $(OH)_2$ to MgO. For $Fe_3O_4$ weight loss below 320 °C is due to the loss of physically adsorbed water. The weight loss from 320 °C to 450 °C is ascribed to the loss of oxygen-containing functional groups. The TGA curve of $Fe_3O_4$-MgO reveals the weight loss of physisorbed water at low temperatures (25°C -200°C) and chemisorbed water at high temperature (200°C -500°C). The weight loss of functionalized $Fe_3O_4$NPs occurs not only from physically and chemically adsorbed water but also from the loss of the organic layers on $Fe_3O_4$NPs surface Thus these metal oxide nanoparticles and composite materials showed gradual weight loss with increasing temperature till 400 after that there is no loss of weight.

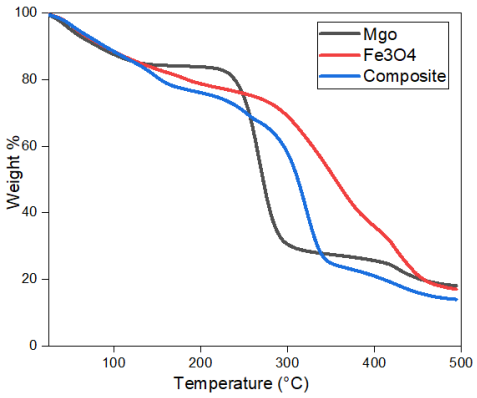


**Fig 5.** TGA curves of MgO, $Fe_3O_4$NPs and $Fe_3O_4$-MgO nanocomposite

## 3.6 Cytotoxicity measurement by hemolytic assay

All the drugs when enter into the blood and get associated with red blood cells, it is important that prepared nanomaterials should be subjected to biocompatibility testing to study the toxicity on blood erythrocytes before performing the antioxidant activity. The initial assessment of the biocompatibility of MgO, $Fe_3O_4$ NPs and $Fe_3O_4$-MgO nanocomposite was carried out by using hemolytic assay and the results obtained are 1.8%, 2.2% and 1.4% respectively. According to the ISO/TR 7406 the biocompatible range is $\leq$ 5% is nontoxic to the blood erythrocytes [20]. Our results display that, all synthesized nanomaterials shown less than 5% hemolytic activity and $Fe_3O_4$-MgO nanocomposite exhibit overall more compatible with erythrocytes when compared to the MgO and $Fe_3O_4$NPs. Therefore, it may be stated that the synthesized nanomaterials are biocompatible in nature at its lower concentration.

## 3.7 Antioxidant Activity (AOA)

The antioxidant activity of LPE-mediated synthesized nonmaterials was carried out against DPPH as a free radical model and water as control. The result indicated that $Fe_3O_4$-MgO composite showed remarkable antioxidant activity. The scavenging activity of the metal oxide NPs were increased in a dose dependent manner. The increase in the quantity of $Fe_3O_4$-MgO nanocomposite from 20, 40, 60, 80 and 100 $\mu$g/mL, DPPH scavenging activity increases as 44.45, 62.24, 71.28, 80.96 and 89.95%, respectively. It is assumed, that LPE phytochemicals quench ROS which are available on the spherical surface of $Fe_3O_4$-MgO nanocomposites and its ensuing effect on the antioxidant agent's action. Due to the involvement of free radicals in various pathologies, the search for novel molecules capable of overcoming the deficiency of the endogenous defense system has been greatly enhanced. Antioxidant capacity can only be measured indirectly by its effects. Most methods of measuring antioxidant activity rely on the use of systems that generate a variety of free radicals. Essentially, these are called 'inhibition' methods where chemicals capable of generating free radicals are used in conjunction with a substance capable of detecting these types [21]. The DPPH free radical scavenging assay (%) and half-maximal inhibitory concentration ($IC_{50}$) of prepared metal oxide nanoparticles and nanocomposites are presented in Figure 6 (a and b). The DPPH free radical scavenging rate of the MgO nanoparticles showed lowest antioxidant activity among all the synthesized nanomaterials, probably due to the interactions of free radicals and free amino groups present in the extract. But, in the case of $Fe_3O_4$ NPs the DPPH scavenging activity increased inhibition of free radicals by the function of an increased concentration. Particularly, the nanocomposite containing a high concentration of $Fe_3O_4$-MgO exhibited higher DPPH radical scavenging activity. The antioxidant activity of nanocomposite occurs due to the more abundant phenolic hydroxyl groups present in their structure making them to capture

free radicals by donating phenolic hydrogen atoms. The half-maximal inhibitory concentration ($IC_{50}$) of the entire synthesized nanocomposite was determined (in $\mu$g/mL). Strong, moderate and weak antioxidants were defined as those with an $IC_{50}$ value between 10 and 50, 50–100, and > 100 $\mu$g/mL, respectively[22]. The $IC_{50}$ value of $Fe_3O_4$-MgO nanocomposite was found to be remarkably similar $IC_{50}$ value of standard ascorbic acid. This indicates that, the prepared nanocomposite functioned as more effective in antioxidant properties. Table 1 represents some important reports of nanoparticles and nanocomposites decorated with metal/metal oxide, that were compared with the present work, which suggests that, the present prepared active nanocomposites showed very good antioxidant properties compared to the others reported work.

**Table 1.** The literature comparison of antioxidant activity of nanocomposites with present work

| Material Composition | Antioxidant | |
|---|---|---|
| $Fe_3O_4$/CuO | 30.28% | [23] |
| PFu/ $Fe_3O_4$ | 49.45% | [24] |
| GO/MgO | 56.71% | [25] |
| CuO/MgO | 59.62% | [26] |
| Au/MgO | 82.58% | [27] |
| $Fe_3O_4$/MgO | 89.95% | Present work |

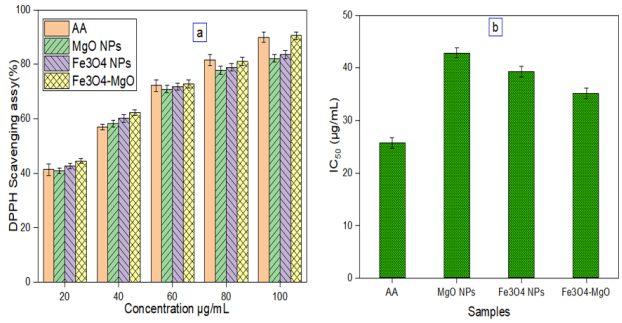


**Fig 6.** Antioxidant profile (**a**) and $IC_{50}$ value of prepared MgO, $Fe_3O_4$ NPs and $Fe_3O_4$-MgO nanocomposites (**b**) (mean ± SD) (AA=Ascorbic acid)

## 3.8 Antibacterial activity

The antibacterial activities of nanoparticles were tested against gram positive bacteria (*S. aureus and S. mutans*) and gram negative (*E.coli & K. pneumonia*). From the antimicrobial assay, it was observed that the MgO, $Fe_3O_4$ NPs and $Fe_3O_4$-MgO have hostile effect on the growth of all these grams negative and gram positive bacteria as shown in Figure 7. It is observed that $Fe_3O_4$-MgO composite possess the highest antibacterial activity and $Fe_3O_4$and MgO NPs exhibit moderate and least activity respectively against various bacteria (Table 2). Metal ions, metal complexes, and quaternary ammonium compounds are some of the antibacterial agents that are used commercially. It has been claimed that these substances have numerous drawbacks, such as antibiotic resistance and high cost. Metal oxide nanocomposite is an efficient antibacterial agent due to its ease of manufacture, affordability, and environmental sustainability. The metal oxide NPs overcome microbial drug resistance by rupturing bacterial cell membrane, making them effective antibacterial agents[28].

**Table 2.** Zone of inhibition ofMgO, $Fe_3O_4$ and $Fe_3O_4$-MgO NPs against different bacterial strains

| Samples | Zone of Inhibition Diameter (mm) | | Zone of Inhibition Diameter (mm) | |
|---|---|---|---|---|
| | ***E. Coli*** | ***K . pneumonia*** | ***Streptococcus mutans*** | ***S. Aureus*** |
| $Fe_3O_4$-MgO **(A)** | 23 | 21 | 25 | 12 |
| $Fe_3O_4$ NPs **(B)** | 21 | 18 | 21 | 13 |
| MgO NPs **(C)** | 20 | 09 | 23 | 16 |
| Standard | 33 | 26 | 36 | 27 |
| control | 00 | 00 | 00 | 00 |

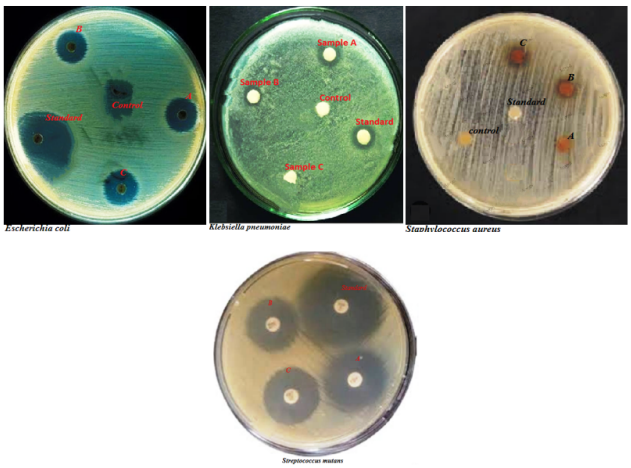


**Fig 7.** Antimicrobial activity of MgO, $Fe_3O_4$ and $Fe_3O_4$-MgO NPs against; *E. coli, K. pneumonia, S. aureus and S. mutans*

## 4 Conclusion

This study presents the green synthesis of MgO, $Fe_3O_4$ NPs and $Fe_3O_4$-MgO nanocomposite using lemon peel extract. The prepared iron and magnesium oxide nanoparticles showed good antioxidant activities against DPPH (less than 85%) but $Fe_3O_4$-MgO nanocomposite showed remarkable antioxidant activity (89.95%). Antibacterial investigations showed that the nanomaterials were capable of eradicating both gram-positive and gram-negative bacteria ($IC_{50}$ value are 8.32, 8.15 & 8.13 and 7.23, 7.57 & 7.47 $\mu$g/mL respectively). As a result, the use of agricultural waste such as lemon peel in nanoscience offers a sustainable, low-cost, non-toxic and eco-friendly solution. Thus, this study confirmed that the lemon peel extract derived $Fe_3O_4$-MgO nanocomposites can be used as an effective antioxidant and antibacterial agent in biomedical applications.

### Acknowledgement

The work was financially supported by Karnataka DST-Ph.D. fellowship of Department of Science and Technology (DST), Govt. of Karnataka. (No: DST/KSTePS/Ph.D fellowship/CHE-05:2020-21) KSTePS, DST, Government of Karnataka, Bangalore to the first author. PMG thanks to VGST (GRD 503 & 952) and Rani Channamma University for Minor research project 2020 & 2021.

## References

1) Nabi G, Qurat-Ul-Aain, Khalid NR, Tahir MB, Rafique M, Rizwan M, et al. A Review on Novel Eco-Friendly Green Approach to Synthesis TiO2 Nanoparticles Using Different Extracts. *Journal of Inorganic and Organometallic Polymers and Materials*. 2018;28(4):1552–1564. Available from: https://doi.org/10.1007/s10904-018-0812-0.
2) Nabi G, Ain QUU, Tahir MB, Riaz KN, Iqbal T, Rafique M, et al. Green synthesis of TiO2 nanoparticles using lemon peel extract: their optical and photocatalytic properties. *International Journal of Environmental Analytical Chemistry*. 2022;102(2):434–442. Available from: https://doi.org/10.1080/03067319.2020.1722816.
3) Balaba N, Jaerger S, Horsth DFL, Primo JDO, Correa JDS, Bittencourt C, et al. Polysaccharides as Green Fuels for the Synthesis of MgO: Characterization and Evaluation of Antimicrobial Activities. *Molecules*. 2023;28(1):142. Available from: https://doi.org/10.3390/molecules28010142.
4) Saikia JP, Paul S, Konwar BK, Samdarshi SK. Nickel oxide nanoparticles: A novel antioxidant. *Colloids and Surfaces B: Biointerfaces*. 2010;78(1):146–148. Available from: https://doi.org/10.1016/j.colsurfb.2010.02.016.
5) Banerjee S, Saikia JP, Kumar A, Konwar BK. Antioxidant activity and haemolysis prevention efficiency of polyaniline nanofibers. *Nanotechnology*. 2010;21(4):045101. Available from: https://doi.org/10.1088/0957-4484/21/4/045101.
6) Anjana VN, Joseph M, Francis S, Joseph A, Koshy EP, Mathew B. Microwave assisted green synthesis of silver nanoparticles for optical, catalytic, biological and electrochemical applications. *Artificial Cells, Nanomedicine, and Biotechnology*. 2021;49(1):438–449. Available from: https://doi.org/10.1080/21691401.2021.1925678.
7) Prasad C, Sreenivasulu K, Gangadhara S, Venkateswarlu P. Bio inspired green synthesis of Ni/Fe3O4 magnetic nanoparticles using Moringa oleifera leaves extract: A magnetically recoverable catalyst for organic dye degradation in aqueous solution. *Journal of Alloys and Compounds*. 2017;700:252–258. Available from: https://doi.org/10.1016/j.jallcom.2016.12.363.

8) Sajadi SM, Nasrollahzadeh M, Maham M. Aqueous extract from seeds of Silybum marianum L. as a green material for preparation of the Cu/Fe3O4 nanoparticles: A magnetically recoverable and reusable catalyst for the reduction of nitroarenes. *Journal of Colloid and Interface Science*. 2016;469:93–98. Available from: https://doi.org/10.1016/j.jcis.2016.02.009.
9) Lagashetty A, Ganiger SK, K PR, Reddy S, Pari M. Microwave-assisted green synthesis, characterization and adsorption studies on metal oxide nanoparticles synthesized using Ficus Benghalensis plant leaf extracts. *New Journal of Chemistry*. 2020;44(33):14095–14102. Available from: https://doi.org/10.1039/D0NJ01759K.
10) Shinde G, Thakur J. Core-shell structured Fe3O4@MgO: magnetically recyclable nanocatalyst for one-pot synthesis of polyhydroquinoline derivatives under solvent-free conditions. *Journal of Chemical Sciences*. 2023;135(1):14. Available from: https://doi.org/10.1007/s12039-023-02134-9.
11) Panchal P, Paul DR, Sharma A, Hooda D, Yadav R, Meena P, et al. Phytoextract mediated ZnO/MgO nanocomposites for photocatalytic and antibacterial activities. *Journal of Photochemistry and Photobiology A: Chemistry*. 2019;385:112049. Available from: https://doi.org/10.1016/j.jphotochem.2019.112049.
12) Patiño-Ruiz DA, Meramo-Hurtado SI, Ángel Dario González-Delgado, Herrera A. Environmental Sustainability Evaluation of Iron Oxide Nanoparticles Synthesized via Green Synthesis and the Coprecipitation Method: A Comparative Life Cycle Assessment Study. *ACS Omega*. 2021;6(19):12410–12423. Available from: https://doi.org/10.1021/acsomega.0c05246.
13) Neun BW, Ilinskaya AN, Dobrovolskaia MA. Updated method for in vitro analysis of nanoparticle hemolytic properties. 2018. Available from: https://doi.org/10.1007/978-1-4939-7352-1_9.
14) Roy D, Pal A, Pal T. Electrochemical aspects of coinage metal nanoparticles for catalysis and spectroscopy. *RSC Advances*. 2022;12(19):12116–12135. Available from: https://doi.org/10.1039/D2RA00403H.
15) Pugazhendhi A, Prabhu R, Muruganantham K, Shanmuganathan R, Natarajan S. Anticancer, antimicrobial and photocatalytic activities of green synthesized magnesium oxide nanoparticles (MgONPs) using aqueous extract of Sargassum wightii. *Journal of Photochemistry and Photobiology B: Biology*. 2019;190:86–97. Available from: https://doi.org/10.1016/j.jphotobiol.2018.11.014.
16) Ramesh R, Geerthana M, Prabhu S, Sohila S. Synthesis and Characterization of the Superparamagnetic Fe3O4/Ag Nanocomposites. *Journal of Cluster Science*. 2017;28(3):963–969. Available from: https://doi.org/10.1007/s10876-016-1093-9.
17) Priyadarshini B, Patra T, Sahoo TR. An efficient and comparative adsorption of Congo red and Trypan blue dyes on MgO nanoparticles: Kinetics, thermodynamics and isotherm studies. *Journal of Magnesium and Alloys*. 2021;9(2):478–488. Available from: https://doi.org/10.1016/j.jma.2020.09.004.
18) Kurnaz YN, Kurşun BF, Koç MM, Nartop D. Characterization of magnetic Fe3O4@ SiO2 nanoparticles with fluorescent properties for potential multipurpose imaging and theranostic applications. *Journal of Materials Science: Materials in Electronics*. 2020;31(20):18278. Available from: https://doi.org/10.1007/s10854-020-04375-7.
19) Chowdhury AH, Ghosh S, Islam SM. Flower-like AgNPs@m-MgO as an excellent catalyst for CO2 fixation and acylation reactions under ambient conditions. *New Journal of Chemistry*. 2018;42(17):14194–14202. Available from: https://doi.org/10.1039/C8NJ02286K.
20) Anigol LB, Sajjan VP, Gurubasavaraj PM, Ganachari SV, Patil D. Study on the effect of pH on the biosynthesis of silver nanoparticles using Capparis moonii fruit extract: their applications in anticancer activity, biocompatibility and photocatalytic degradation. *Chemical Papers*. 2023;77(6):3327–3345. Available from: https://doi.org/10.1007/s11696-023-02707-5.
21) Meresht AS, Ezzatzadeh E, Dehbandi B, Salimifard M, Rostamian R. Fe3O4 CuO Nanocomposite Promoted Green Synthesis of Functionalized Quinazolines Using Water Extract ofLettuce Leavesas Green Media: Study of Antioxidant Activity. *Polycyclic Aromatic Compounds*. 2022;42(7):4793–4808. Available from: https://doi.org/10.1080/10406638.2021.1913426.
22) Zare EN, Lakouraj MM, Baghayeri M. Electro-Magnetic Polyfuran/Fe3O4 Nanocomposite: Synthesis, Characterization, Antioxidant Activity, and Its Application as a Biosensor. *International Journal of Polymeric Materials and Polymeric Biomaterials*. 2015;64(4):175–183. Available from: https://doi.org/10.1080/00914037.2014.936588.
23) Fathy RM, Mahfouz AY. Eco-friendly graphene oxide-based magnesium oxide nanocomposite synthesis using fungal fermented by-products and gamma rays for outstanding antimicrobial, antioxidant, and anticancer activities. *Journal of Nanostructure in Chemistry*. 2021;11(2):301–321. Available from: https://doi.org/10.1007/s40097-020-00369-3.
24) Krishnan SG, Pravitha S. A comparative study on the antioxidant activity of CuO/MgO nanocomposites synthesized via chemical and biological route. *AIP Conference Proceedings*. 2020;2244:70033. Available from: https://doi.org/10.1063/5.0009320.
25) Khan AU, Khan QU, Tahir K, Ullah S, Arooj A, Li B, et al. A Tagetes minuta based eco-benign synthesis of multifunctional Au/MgO nanocomposite with enhanced photocatalytic, antibacterial and DPPH scavenging activities. *Materials Science and Engineering: C*. 2021;126:112146. Available from: https://doi.org/10.1016/j.msec.2021.112146.
26) Gulcin I. Antioxidants and antioxidant methods: an updated overview. *Archives of Toxicology*. 2020;94(3):651–715. Available from: https://doi.org/10.1007/s00204-020-02689-3.
27) Amaregouda Y, Kamanna K, Gasti T. Fabrication of intelligent/active films based on chitosan/polyvinyl alcohol matrices containing Jacaranda cuspidifolia anthocyanin for real-time monitoring of fish freshness. *International Journal of Biological Macromolecules*. 2022;218:799–815. Available from: https://doi.org/10.1016/j.ijbiomac.2022.07.174.
28) Mishra A, Pradhan D, Halder J, Biswasroy P, Rai VK, Dubey D, et al. Metal nanoparticles against multi-drug-resistance bacteria. *Journal of Inorganic Biochemistry*. 2022;237:111938. Available from: https://doi.org/10.1016/j.jinorgbio.2022.111938.